Effect of Pressure on the Self-Exchange Velocities in MD Simulations of Molten LiCl and LiBr Reflecting the Anomaly in the Conductivities

Isao Okada, Akira Endoh*, and Shipra Baluja

Department of Electronic Chemistry, Tokyo Institute of Technology, Nagatsuta 4259, Midori-ku, Yokohama 227, Japan

Z. Naturforsch. **46a**, 148–154 (1991); received May 25, 1990

This paper is dedicated to Dr. Karl Heinzinger on the occasion of his 60th birthday

In molecular dynamics simulations of molten LiCl and LiBr at about 1000 K and various pressures the self-exchange velocity of unlike ion pairs divided by the molar volume increases with increasing pressure up to ca. 1000 MPa, reflecting the trend experimentally found for the electric conductivity up to 100 MPa. While the coordination of unlike ions is tetrahedral at low pressures, it is nearly octahedral at 2000 MPa.

Introduction

Cleaver et al. [1] have found that the conductivity $\varkappa = Fb/V$ (b: internal mobility, V: molar volume, F: Faraday constant) of molten LiCl, LiBr and LiI increases with increasing pressure (0.1–100 MPa). Further, Tödheide and his coworkers have found that the molar conductivity $\Lambda = Fb$ of molten LiBr in the range from 993 to 1313 K goes through a maximum as a function of pressure (0–600 MPa), which has been interpreted in terms of the high polarizing power of Li^+ [2].

We have found that the self-exchange velocity (SEV), v, calculated from molecular dynamics (MD) simulations, is strongly correlated with b [3–6]. We previously calculated v of molten KCl at 1173 K under high pressures and found that v/V decreases with increasing pressure [7], as does b/V [8, 9].

In the present MD study we have calculated v/V of molten LiCl and LiBr at various pressures in order to compare the results with those of [1] and [2] and to reach a better understanding of the process.

* Present address: Fujitsu Laboratories Ltd., Morinosato-Wakamiya 10-1, Atsugi-shi 243-01, Japan.

Reprint requests to Professor Isao Okada, Department of Electronic Chemistry, Tokyo Institute of Technology, Nagatsuta, Midori-ku, Yokohama 227, Japan.

MD Simulation

432 ions were disposed in the periodic cell. The density at each pressure was determined by the equation [10],

$$\varrho(P, T) = \varrho(P_0, T)/\{1 - 0.1 \ln[(0.089/\beta_T(P_0, T) + 4.0 \times 10^6 + P)/(0.089/\beta_T(P_0, T) + 4.0 \times 10^6)]\}, \quad (1)$$

where $\varrho(P, T)$ is the density of the melt at the pressure P (Pa) and the temperature T (K), P_0 is a reference pressure ($P_0 = 1.0 \times 10^5$ Pa) [11] and $\beta_T(P_0, T)$ is the isothermal compressibility at P_0 and T [12]. From the density, V at 1000 K and the edge length L of the cubic MD cell were calculated for each prescribed pressure P_p.

The pair potentials were of the Born-Mayer-Huggins type with the Tosi-Fumi parameters [13]. After about 5000 time steps at constant temperature for equilibration, the MD runs were performed for another 5000 time steps by a constant energy method.

Results and Discussion

Thermodynamic Properties

Some conditions and results of the MD simulations are summarized in Table 1. P_c was calculated from the virial resulting from the simulation [14]. When the Tosi-Fumi parameters [13] are employed for the simu-

0932-0784 / 91 / 0100-0148 $ 01.30/0. – Please order a reprint rather than making your own copy.

Table 1. Prescribed pressure P_p, molar volume V, edge length L, calculated pressure P_c, temperature T, and potential energy E for molten LiCl and LiBr.

P_p/MPa	V/cm^3 mol^{-1}	L/pm	P_c/MPa	T/K	E/kJ mol^{-1}
LiCl					
0.1	29.21	2187.9	220	1007	−796.8
200	28.02	2157.8	460	998	−798.0
500	26.84	2127.1	740	983	−799.6
1000	25.55	2092.4	1180	1002	−800.2
2000	23.97	2048.5	1970	1011	−800.6
LiBr					
0.1	35.98	2345.3	210	1003	−747.0
200	34.30	2308.2	380	999	−748.2
500	32.70	2271.7	680	988	−749.7
1000	31.01	2232.0	1100	1009	−750.4
2000	29.00	2182.7	1810	999	−751.2

lation of molten salts whose densities are experimentally determined under ambient pressure, P_c is usually of the order 200 MPa (e.g. $P_c = 160$ MPa for KCl at 1173 K, when $P_p = 0.1$ MPa [7]). The P_c's were systematically higher than P_p by about 200 MPa except in the case of $P_p = 2000$ MPa.

The calculated potential energy E decreases slightly with pressure. Since the unlike-ion distance does not vary much, the increase in pressure leads to higher values of both the Coulombic and repulsion energies [15], which compensate each other, resulting in no marked effect on the values of the potential energies.

The isothermal compressibility was calculated to be 1.6×10^{-10} Pa^{-1} for LiCl and 2.7×10^{-10} Pa^{-1} for LiBr.

Pair Correlation Functions and Coordination Numbers

Some characteristic values of the pair correlation functions $g(r)$ are given in Tables 2 and 3. From these tables it is seen that for unlike ions and increasing pressure R_M and R_2 do not change appreciably while $g(R_M)$ decreases, showing that with increasing pressure the increase of the overall density is greater than the increase of the density in the first coordination sphere. For like ions and increasing pressure R_M and R_2 decrease and $g(R_M)$ increases. These trends are in agreement with those observed for molten KCl [7] and for molten (Li, K)Cl of the eutectic composition [15]. Figure 1 shows that for unlike ions the running coordination number $n(r)$ increases with increasing pressure, as expected. R_2 is regarded as the radius of the first coordination sphere [16] and defines the coordination number $n(R_2)$. For unlike ions $n(R_2)$ increases with pressure.

Table 2. Characteristic values of the pair correlation functions for molten LiCl. R_1 and R_2 are the distances where $g_{ij}(r)$ crosses unity for the first and the second time, respectively. R_M and R_m are the distances at the first maximum and the first minimum, respectively.

P_p/MPa	0.1	200	500	1000	2000
Li–Li					
R_1/pm	318	316	315	311	307
R_M/pm	371	370	369	365	357
$g(R_M)$	1.82	1.83	1.85	1.86	1.89
R_2/pm	459	457	454	452	447
R_m/pm	535	530	530	530	525
Cl–Cl					
R_1/pm	324	322	321	318	314
R_M/pm	373	369	363	359	355
$g(R_M)$	2.13	2.15	2.18	2.24	2.29
R_2/pm	455	451	449	445	438
R_m/pm	537	525	525	520	520
Li–Cl					
R_1/pm	192	193	193	194	194
R_M/pm	223	223	223	223	223
$g(R_M)$	3.72	3.66	3.58	3.46	3.39
R_2/pm	281	281	281	282	282
$n(R_2)$	3.09	3.18	3.27	3.40	3.56
R_m/pm	353	350	350	350	350

Table 3. Characteristic values of the pair correlation functions for molten LiBr. See also the legend of Table 2.

P_p/MPa	0.1	200	500	1000	2000
Li–Li					
R_1/pm	341	339	336	332	327
R_M/pm	397	396	395	392	381
$g(R_M)$	1.79	1.80	1.82	1.82	1.84
R_2/pm	494	492	488	485	479
R_m/pm	573	565	565	560	560
Br–Br					
R_1/pm	348	347	343	340	336
R_M/pm	401	396	393	389	381
$g(R_M)$	2.14	2.16	2.22	2.28	2.34
R_2/pm	487	486	481	476	467
R_m/pm	573	565	560	560	550
Li–Br					
R_1/pm	207	208	209	209	209
R_M/pm	239	239	240	240	240
$g(R_M)$	3.78	3.64	3.58	3.45	3.39
R_2/pm	302	303	303	303	304
$n(R_2)$	3.10	3.21	3.31	3.45	3.67
R_m/pm	369	370	370	370	370

The percentages of specific coordination numbers of Cl^- and Br^- around Li^+ are shown in Table 4. The

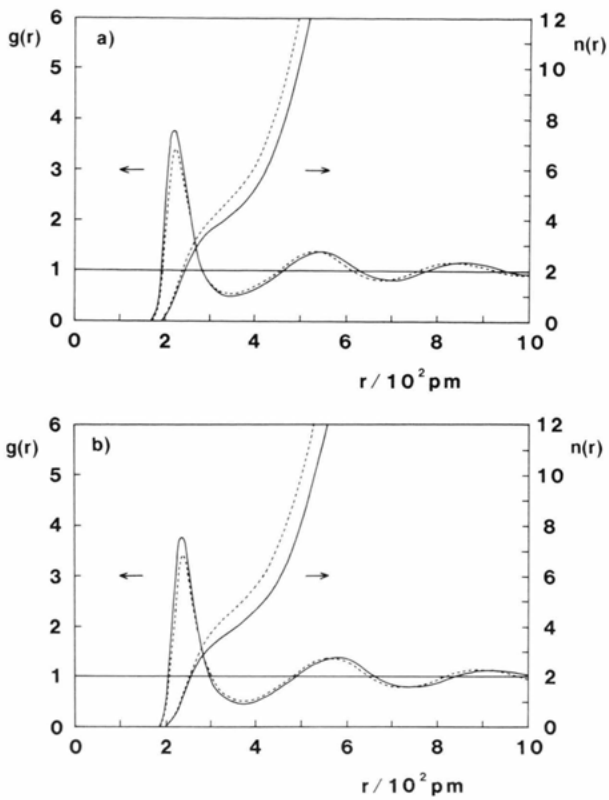

Fig. 1. Pair correlation functions between unlike ions $g(r)$ and the running coordination numbers $n(r)$ for (a) LiCl and (b) LiBr. ——: $P_p = 0.1$ MPa, – – –: $P_p = 2000$ MPa.

percentages of the specific coordination numbers 4, 5, and 6 increase with increasing pressure. When P_p changes from 1000 MPa to 2000 MPa, the most probable specific coordination number changes from 3 to 4.

Angular Correlation Function

The angular correlation function $P_{-+-}(\cos\theta)$ is defined by

$$P_{-+-}(\cos\theta) = -C\, \mathrm{d}n(\cos\theta)/\mathrm{d}(\cos\theta), \tag{2}$$

where θ is the angle formed by two anions in the first coordination sphere with respect to the central cation, and where C is a normalization factor chosen so that

$$\int_{-1}^{1} P_{-+-}(\cos\theta)\, \mathrm{d}(\cos\theta) = 1. \tag{3}$$

$P_{-+-}(\cos\theta)$ and $P_{+-+}(\cos\theta)$ for LiCl are shown in Fig. 2, and those for LiBr in Figure 3. $P_{+-+}(\cos\theta)$ at $P_p = 0.1$ MPa for LiCl is in good agreement with that shown in Figure 2 of [4].

Table 4. Distribution of the numbers of neighbouring anions around Li^+ within R_2 at different pressures in molten LiCl and LiBr (in percent).

P_p/MPa	n						
	0	1	2	3	4	5	6
LiCl							
0.1	0	0.68	16.95	55.98	25.45	0.93	0.01
200	0	0.57	14.53	54.20	29.41	1.28	0.01
500	0	0.42	11.81	51.84	34.02	1.89	0.02
1000	0	0.28	8.98	47.33	39.85	3.52	0.04
2000	0	0.17	6.91	40.26	46.59	6.61	0.18
LiBr							
0.1	0.01	0.72	16.48	55.52	26.34	0.92	0.01
200	0.01	0.60	13.99	52.94	30.86	1.58	0.02
500	0	0.39	10.99	50.10	36.11	2.38	0.03
1000	0	0.28	8.12	44.84	42.18	4.48	0.10
2000	0	0.10	4.63	35.83	50.13	8.98	0.33

The peak positions of P_{-+-} and P_{+-+} for LiCl and LiBr are given in Table 5. P_{-+-} has one peak around 101° at $P_p = 0.1$ MPa and two peaks around 94° and 180° at 2000 MPa both for LiCl and LiBr. P_{+-+} has maxima at similar angles. This suggests that with increasing pressure a nearly regular tetrahedral arrangement of Cl^- around Li^+ (although $n(R_2) < 4$) changes to a nearly octahedral one, i.e. the NaCl-type structure (although $n(R_2) < 6$).

It should be mentioned, however, that according to very recent neutron diffraction measurements, analyzed by the reverse Monte Carlo method, molten LiCl shows octahedral symmetry at ambient pressure [17], whereas all other results by neutron and X-ray diffraction support tetrahedral symmetry. This discrepancy needs clarification.

Self-Exchange Velocity

The SEV, v, is defined as [3]

$$v = (R_2 - \bar{r}_{R_2})/\tau, \tag{5}$$

where $\bar{r}_{R_2}$ is the average distance of the counterions within the distance R_2 from the ion and τ is the time at which the average distance of these counterions becomes R_2.

We have found that the internal mobility is approximately proportional to the SEV [3–6]:

$$\Lambda/F = b \cong k' v, \tag{6}$$

$$\varkappa/F = b/V \cong k' v/V, \tag{7}$$

where k' is a constant.

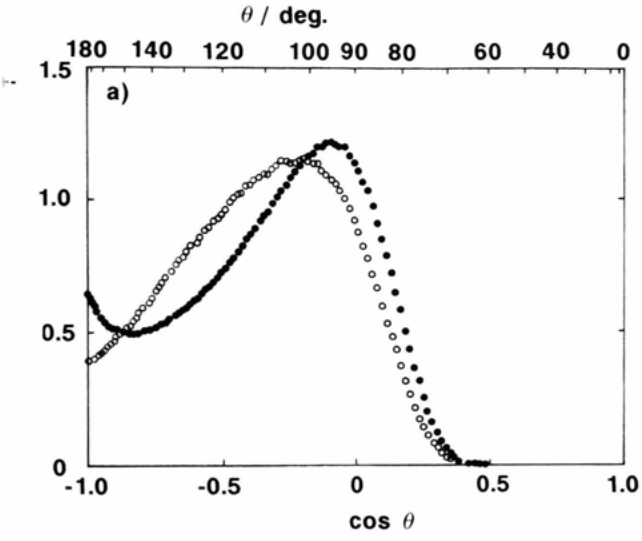

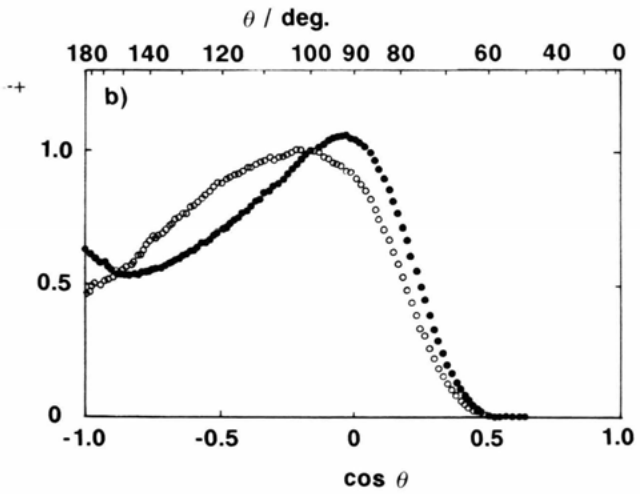

Fig. 2. Angular correlation functions (a) $P_{-+-}(\cos\theta)$ and (b) $P_{+-+}(\cos\theta)$ for LiCl. ○: $P_p = 0.1$ MPa, ●: 2000 MPa.

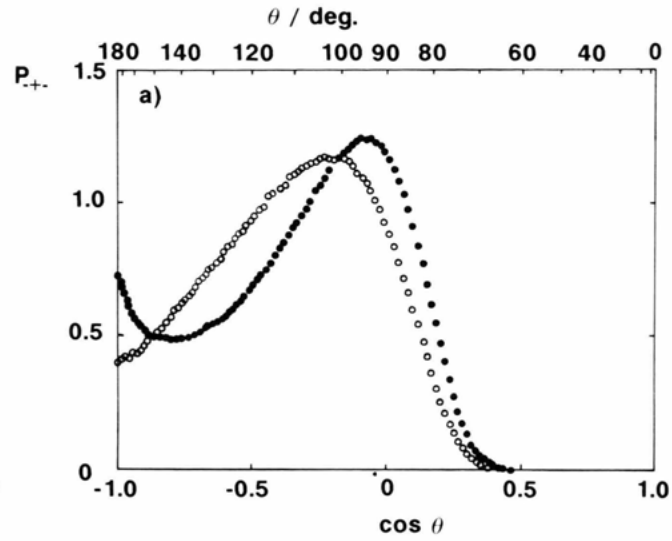

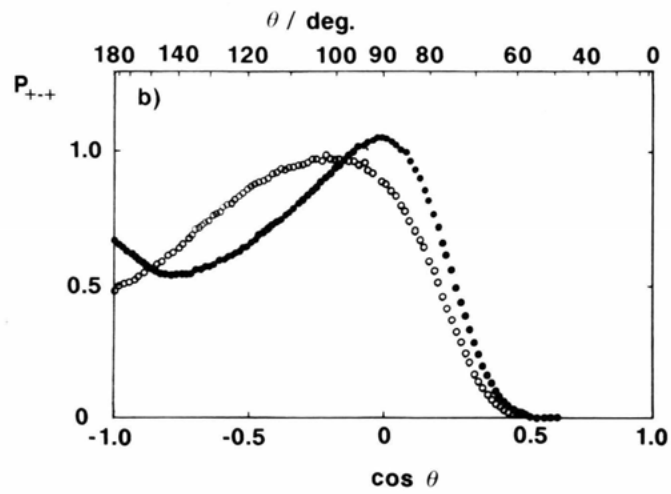

Fig. 3. Angular correlation functions (a) $P_{-+-}(\cos\theta)$ and (b) $P_{+-+}(\cos\theta)$ for LiBr. ○: $P_p = 0.1$ MPa, ●: 2000 MPa.

Table 5. Angles (in degrees) at the maxima of the angular correlation functions $P_{-+-}(\cos\theta)$ and $P_{+-+}(\cos\theta)$ for LiCl and LiBr.

P_p/MPa	LiCl		LiBr	
	P_{-+-}	P_{+-+}	P_{-+-}	P_{+-+}
0.1	100	101	102	102
200	101	99	100	98
500	99, ~175	96, ~176	98, ~173	96, ~176
1000	96, ~174	97, ~174	95, ~177	92, ~173
2000	94, ~176	91, ~176	94, ~177	91, ~176

The calculated values of v and v/V are given in Table 6. For LiBr, v is the same at $P_p = 0.1$ and 200 MPa, which reflects the experimental result [2] that at 993 K Λ has a slight maximum at about 200 MPa in the range 0.1 to 300 MPa. At all other places in Table 6 v smoothly decreases with increasing pressure while v/V increases up to $P_p = 1000$ MPa. This reflects the experimental finding [1] that in the range 0.1 – 100 MPa $\varkappa$ of LiCl and LiBr increases with pressure.

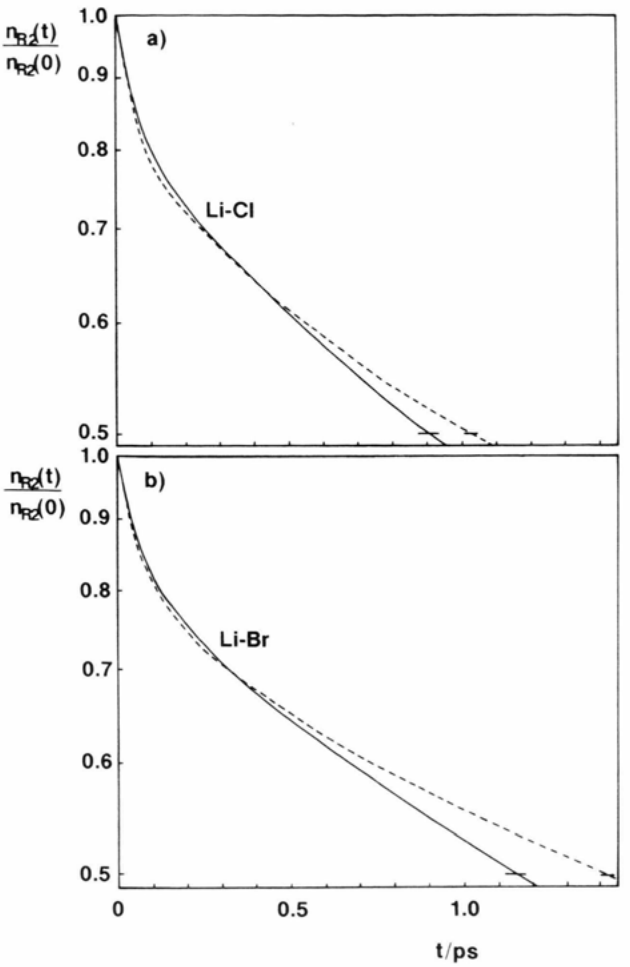

Fig. 4. Time evolution of $n_{R_2}(t)/n_{R_2}(0)$. (a) LiCL, (b) LiBr. The solid and dashed lines are for $P_p = 0.1$ MPa and 2000 MPa, respectively. The ordinate is logarithmically scaled.

Another measure for the separating motion of neighbouring unlike ion pairs is the decrease of the number of marked counter ions present within the coordination sphere [3]. This number is referred to as $n_{R_2}(t)$, and the time evolution of $n_{R_2}(t)/n_{R_2}(0)$ is shown for $P_p = 0.1$ MPa and 2000 MPa in Figure 4. At the beginning this quantity declines more quickly for $P_p = 2000$ MPa than for $P_p = 0.1$ MPa, whereas later the reverse is true. $\tau_{1/2}$, the half life of $n_{R_2}(t)$, and v are anticorrelated, as shown in Figure 5.

The isothermal activation volumes of Λ and $\varkappa$ are given by

$$\Delta V_\Lambda = -RT(\partial \ln \Lambda/\partial P)_T \quad \text{and} \tag{8}$$

$$\Delta V_\varkappa = -RT(\partial \ln \varkappa/\partial P)_T, \tag{9}$$

respectively.

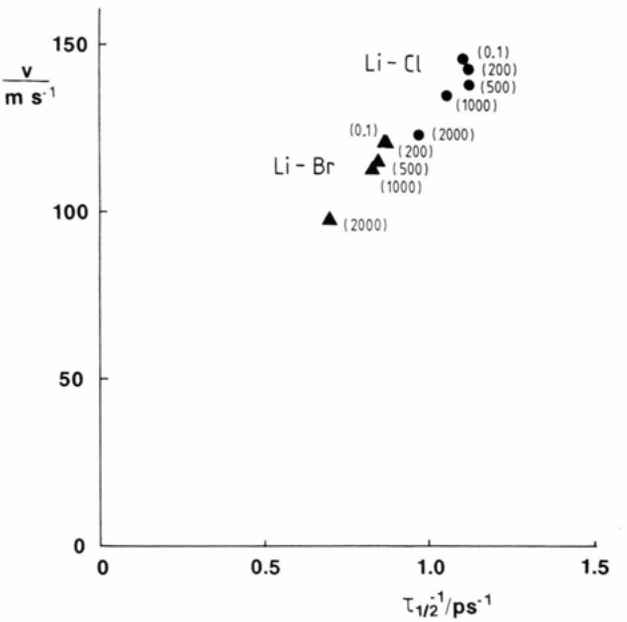

Fig. 5. Relationship between $\tau_{1/2}^{-1}$ and v. ●: LiCl, ▲: LiBr. The figures in parentheses represent P_p in MPa.

Table 6. The self-exchange velocity of neighbouring unlike ions.

P_p/MPa	LiCl		LiBr	
	v/m s^{-1}	$vV^{-1}/10^6$ mol m^{-2} s^{-1}	v/m s^{-1}	$vV^{-1}/10^6$ mol m^{-2} s^{-1}
0.1	146 ± 2	5.00 ± 0.07	121 ± 3	3.36 ± 0.08
200	143 ± 2	5.10 ± 0.07	121 ± 3	3.52 ± 0.09
500	142 ± 2	5.29 ± 0.08	117 ± 2	3.58 ± 0.06
1000	135 ± 2	5.28 ± 0.08	113 ± 3	3.64 ± 0.10
2000	125 ± 2	5.21 ± 0.08	100 ± 1	3.45 ± 0.04

Table 7. The self-diffusion coefficients at about 1000 K and various pressures. The values in parentheses are the experimental ones at ambient pressure.

P_p/MPa	LiCl		LiBr	
	Li	Cl	Li	Br
	$D/10^{-9}$ m^2 s^{-1}			
0.1	11.8 (14.2)	7.4 (7.2) [18]	9.0 (11.7 [a])	5.1 (4.5 [a]) [19]
200	9.2	5.7	8.7	4.7
500	8.0	5.5	7.9	4.2
1000	7.7	5.1	7.6	4.0
2000	7.0	4.5	6.6	2.9

[a] The values for Li^+ and Br^- in LiBr are the self-diffusion coefficients in the mixture of (Li, K) Br (Li: 99 mol%) extrapolated or interpolated to 1000 K.

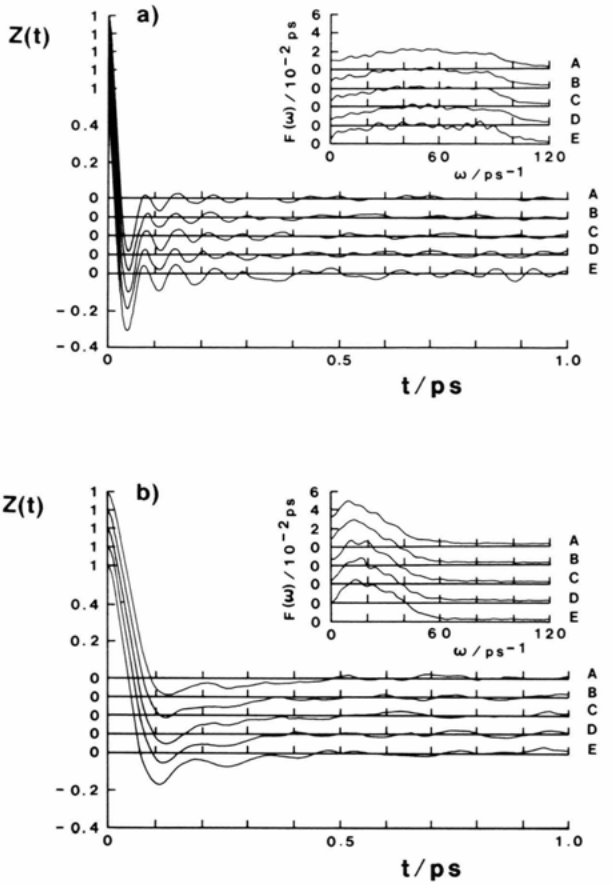

Fig. 6. Velocity autocorrelation functions $Z(t)$ for LiCl. The inset shows the power spectra $F(\omega)$. *A*, *B*, *C*, *D*, and *E* refer to the results at $P_p = 0.1$, 200, 500, 1000, and 2000 MPa, respectively.

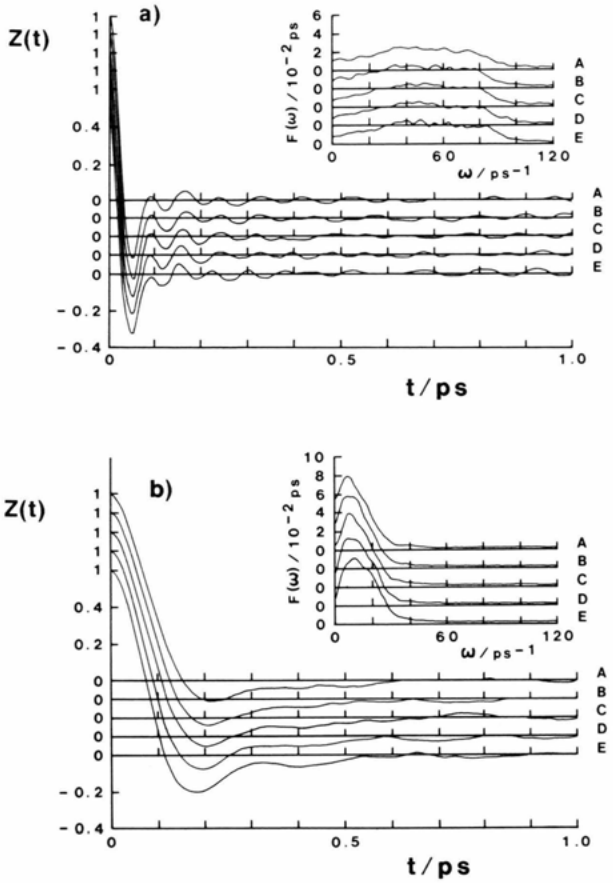

Fig. 7. Velocity autocorrelation functions $Z(t)$ and the power spectra $F(\omega)$ for LiBr. (a) Li^+, (b) Br^-. See also the legend of Fig. 6.

From (6) and (8) follows

$$\Delta V_A \cong \Delta V_v = -RT(\partial \ln v/\partial P_c)_T, \tag{10}$$

and from (7) and (9)

$$\Delta V_\varkappa \cong \Delta V_{(v/V)} = -RT(\partial \ln(v/V)/\partial P_c)_T. \tag{11}$$

ΔV_v calculated from (10) at $P_p = 0.1$ MPa and 200 MPa at 1000 K is 0.7 $cm^3\,mol^{-1}$ for LiCl and 0.0 $cm^3\,mol^{-1}$ for LiBr, while ΔV_A is $(0.4 \pm 0.7)\,cm^3\,mol^{-1}$ for LiCl at 973 K and $(-0.1 \pm 0.4)\,cm^3\,mol^{-1}$ for LiBr at 922 K in the range from 0.1 to 100 MPa [1]. $\Delta V_{(v/V)}$ similarly calculated from (11) is $-1.0\,cm^3\,mol^{-1}$ for LiCl and $-2.3\,cm^3\,mol^{-1}$ at 1000 K for LiBr. These values are in good agreement with the $\Delta V_\varkappa$ values: $-(1.4 \pm 0.7)\,cm^3\,mol^{-1}$ at 973 K for LiCl and $-(1.9 \pm 0.4)\,cm^3\,mol^{-1}$ at 922 K for LiBr [1].

Self-Diffusion Coefficient

For each pressure, the self-diffusion coefficients have been calculated from the mean square displacements which have been taken over 14 ps from 50 different time origins. These values are given in Table 7. The calculated values of LiCl and LiBr agree with those of the experimental results at ambient pressure [18, 19]. The decrease of D with increasing density is greater than the decrease of v (Table 6).

Velocity Autocorrelation Function and Power Spectrum

The velocity autocorrelation functions (VACF) and power spectra are shown for LiCl in Fig. 6 of and for

LiBr in Figure 7. The power spectra are calculated by Fourier transform of the VACF's. With increasing pressure, the depths of the minima of the VACF's become deeper and the VSCF's damp more slowly. This trend is remarkable for the anions. For the anions the first minimum shifts to shorter time with increasing pressure. A similar trend is observed for K^+ and Cl^- in molten (Li, K)Cl of the eutectic composition (see Fig. 4 in [5]). The peak of the power spectra shifts toward higher frequency; this is evident particularly for the anions.

Conclusions

With increase in pressure up to ca. 1000 MPa, the SEV divided by the molar volume increases for molten LiCl and LiBr. This reflects well the anomalous trend experimentally found for the electric conductivity of these melts, although in the simulation polarizations of the ions are not taken account of explicitly but only implicitly by the pair potentials. The slight maximum of the molar conductivity of LiBr in the range 0–600 MPa is reflected by the constancy of the SEV in that range. The coordination for neighbouring unlike ions changes from nearly tetrahedral to octahedral at pressures between ca. 1000 MPa and 2000 MPa at 1000 K.

The MD simulations were performed with the HITAC M-680 H computers at the Institute for Molecular Science (Okazaki) and the National Laboratory for High Energy Physics (Tsukuba). The computer time made available for this work is gratefully acknowledged.

[1] B. Cleaver, S. I. Smedley, and P. N. Spencer, J. Chem. Soc. Faraday Trans. I **68,** 1720 (1972).
[2] K. Tödheide, Angew. Chem. Int. Ed. Engl. **19,** 606 (1980).
[3] I. Okada, R. Takagi, and K. Kawamura, Z. Naturforsch. **35a,** 493 (1980).
[4] I. Okada, Z. Naturforsch. **39a,** 880 (1984).
[5] I. Okada, Z. Naturforsch. **42a,** 21 (1987).
[6] A. Endoh and I. Okada, Z. Naturforsch. **44a,** 1131 (1989).
[7] R. Takagi, I. Okada, and K. Kawamura, Z. Naturforsch. **36a,** 1106 (1981).
[8] R. Schamm, Ph.D. Thesis, Karlsruhe 1978, cited in: B. Cleaver, Advances in Molten Salt Chemistry, vol. 4 (G. Mamantov et al., eds.), Plenum, 1981, p. 71.
[9] R. Schamm, H. P. Vögele, W. Edelbock, and K. Tödheide, High Pressure Sci. Technol., Proc. Int. AIRAPT Conf., 7th, 2 (B. Vodar and P. Mateau, eds.), Pergamon, London 1980, p. 699.
[10] G. Goldmann and K. Tödheide, Z. Naturforsch. **31a,** 769 (1976).
[11] G. J. Janz, C. B. Allen, N. P. Bansal, R. M. Murphy, and R. P. T. Tomkins, Physical Properties Data Compilations Relevant to Energy Storage. II. Molten Salts: Data on Single and Multi-Component Salt Systems, NSRDS-NBS 61, U.S. Dept. Commerce/Nat. Bur. Stand. 1979.
[12] J. O'M. Bockris and N. E. Richards, Proc. Roy. Soc. London **A 241,** 44 (1957).
[13] M. P. Tosi and F. G. Fumi, J. Phys. Chem. Solids **25,** 45 (1964).
[14] L. Schäfer and A. Klemm, Z. Naturforsch. **31a,** 1068 (1976).
[15] F. Lantelme and P. Turq, Z. Naturforsch. **39a,** 162 (1984).
[16] G. Pálinkás, W. O. Riede, and K. Heinzinger, Z. Naturforsch. **32a,** 1137 (1977).
[17] R. L. McGreevy and M. A. Howe, J. Phys.: Condensed Matter **1,** 9957 (1989).
[18] R. Lenke, W. Uebelhack, and A. Klemm, Z. Naturforsch. **28a,** 881 (1973).
[19] M. Chemla, F. Lantelme, and O. P. Mehta, J. Chim. Phys. Spec. No. p. 136 (1969).